Microchimica Acta (2021) 188:267
https://doi.org/10.1007/s00604-021-04935-6

ORIGINAL PAPER

Homogeneous photoelectrochemical biosensor for microRNA based on target-responsive hydrogel coupled with exonuclease III and nicking endonuclease Nb.BbvCI assistant cascaded amplification strategy

Jiao Yang[1] · Shilan Fu[2] · Fang Luo[1] · Longhua Guo[3] · Bin Qiu[1] · Zhenyu Lin[1]

Received: 29 March 2021 / Accepted: 9 July 2021

Abstract

MicroRNAs can serve as biomarkers for many cancers, so it is significant to develop simple and sensitive strategies for microRNAs detection. Photoelectrochemical (PEC) detection has the advantages of simple equipment and high sensitivity. But in conventional PEC DNA sensors, tedious immobilization procedures of photoactive materials and capture probes on electrode surfaces are inevitable. To overcome those limitations, a homogeneous PEC biosensor based on target-responsive hydrogels has been developed (miRNA-155 has been chosen as a model target). PEC signal molecules (TiO_2 nanoparticles, TiO_2 NPs) were embedded in DNA hydrogels formed by hyaluronic acid sodium salt, amine-modified DNA double strands, and polyethylenimine rich in amine groups. In the presence of the target, DNA double strands in hydrogel were nicked by endonuclease and TiO_2 NPs were released to the supernate and a high PEC response was obtained when collecting the supernate for PEC test, while almost no TiO_2 NPs released in the absence of the target. Thanks to the exonuclease III and nicking endonuclease Nb.BbvCI-assisted cascaded amplification strategy, the proposed biosensor exhibits high sensitivity toward miRNA-155 with a low detection limit of 0.41 fM and a wide linear range from 1.0 fM to 100 pM. Since this method circumvents tedious electrode modification procedures, the proposed technique exhibits the advantages of simplicity and good reproducibility. Moreover, the prepared hydrogels have outstanding storage stability, so that they can be prepared in advance and shorten detection time. This biosensing platform provides a versatile strategy for the construction of homogeneous PEC biosensors for the detection of diverse targets.

Keywords Photoelectrochemical biosensor · microRNA · Homogeneous · Target-responsive hydrogel · Signal amplification

Introduction

Abnormal expression of microRNAs (miRNAs) is closely related to the initiation and development of many diseases, such as neurological diseases, cardiovascular diseases, and multiple cancers. [1–3] Classical technologies for miRNA detection includes real-time PCR, [4] northern blotting, [5] and microarray analysis [6]. With the advantages of simple equipment, low background, and high sensitivity, photoelectrochemical (PEC) detection techniques have been applied in the detection of miRNAs frequently. For example, Fu and coworkers prepared a ITO/TiO_2/AuNPs (Au nanoparticles) photoanode by sequential deposition; thiolated complementary DNA was immobilized on the prepared photoanode and conjugated with CdTe quantum dots (QDs) to realize sensitive detection for miRNA-21. [7] Yu and coworkers constructed a PEC sensor

✉ Longhua Guo
guolh@zjxu.edu.cn

✉ Zhenyu Lin
zylin@fzu.edu.cn

[1] Ministry of Education Key Laboratory for Analytical Science of Food Safety and Biology, Fujian Provincial Key Laboratory of Analysis and Detection for Food Safety, College of Chemistry, Fuzhou University, 2 Xue Yuan Road, University Town, Fuzhou, Fujian 350116, People's Republic of China

[2] College of Chemistry and Materials Science, Fujian Normal University, Fuzhou 350117, Fujian, China

[3] College of Biological, Chemical Sciences and Engineering, Jiaxing University, No.56, South Yuexiu Road, Jiaxing 314001, Zhejiang, People's Republic of China

Published online: 22 July 2021

for miRNA-21 based on aptamer/Cu_2MoS_4/In_2O_3-modified electrode through a layer-by-layer assembly strategy and PbS QDs as effective quenchers. [8] However, in those sensors, signal reporting materials and capture probes need to be modified on the electrode first. The spatial hindrance effect on electrode surface brings about the restriction in the configurational freedom of immobilized probes, which can weaken the bio-recognition ability and binding efficiency. [9, 10] Meanwhile, the nonuniformity of electrode modifications will cause low reproducibility. [11, 12] To address these problems, some homogeneous biosensors for miRNAs have been developed. For example, Hou and coworkers utilized the diffusivity difference between methylene blue (MB)-labeled DNA and mononucleotides to develop a modification-free PEC biosensing strategy for miRNA detection. [11] Song and coworkers designed a homogeneous PEC biosensor for miRNA-143 by utilizing the target-induced depletion of electron donors and generation of products with filter effect. [12] Wu and coworkers constructed a homogeneous electrochemical biosensor for miRNA based on the sensitivity for single-stranded DNA and dual enzyme-like activities of a 2D MnO_2 nanoflake. [13] In these works, no complicated layer-by-layer electrode modification was needed. Meanwhile, the bio-recognition and the signal amplification processes happened in homogeneous solutions rather than electrode surfaces, which not only simplified the detection procedures, but also enhanced the bio-recognition efficiency. These studies showed the merits of homogeneous PEC techniques, however, some homogeneous sensing platforms still need the labeling procedures, in addition, how to reduce the background signal to improve the sensitivity of homogeneous biosensors is still a challenge. [14, 15] Consequently, much effort still needs to be paid to explore new effective and simple homogeneous strategies for miRNA detection.

Stimuli-responsive DNA hydrogels usually formed by hybridization of DNA with polymer backbones, which can undergo structure transition in response to external stimuli such as pH, enzymes, ions, and biomolecules. [16, 17] Controlled release systems based on stimuli-responsive DNA hydrogels have been applied to develop biosensors frequently. [18–21] The three-dimensional (3D) network structures of hydrogels are designed to be destroyed in the presence of special target, which results in the releasing of different reporting signal molecules and the released molecules can be detected by different technologies, such as pH, pressure, electrochemical signal, fluorescence signal, and colorimetric signal. [19, 21–26] Those immobilization-free biosensors have the advantages of simpleness, speediness, low background, and easy combination with diverse detection techniques. However, the application of controlled release systems in PEC detection has rarely been reported.

In this study, a homogeneous PEC biosensor for miRNA-155 (chosen as model target) has been developed by utilizing a controlled release system based on TiO_2 nanoparticle (TiO_2 NP)-embedded hydrogels. The TiO_2 NP-loaded hydrogels were prepared owing to the binding of carboxyl groups in hyaluronic acid (HA) and amine groups in polyethylenimine (PEI) and DNA double strands (named DNA bridges). In the presence of the target, the nicking of DNA bridges was induced and caused the breakage of hydrogels and the release of TiO_2 NPs to the supernate, which was collected, and a high photocurrent was obtained. Coupled with a signal amplification strategy based on exonuclease III (Exo III) and nicking endonuclease Nb.BbvCI (Nb.BbvCI), the sensitivity was high enough to determine the target in cancer cells.

Experimental section

Materials and apparatus Hyaluronic acid sodium salt (HA, from *Streptococcus equi*), polyethylenimine (PEI, M.W. 600, 99%), tetrabutyl titanate, 1-ethyl-3-(3-dimethylaminopropyl)-carbodiimide hydrochloride (EDC), and N-hydroxysuccinimide (NHS) were purchased from Aladdin Chemistry Co. (Shanghai, China). Acetonitrile, ethanol and ammonia solution were obtained from Sinopharm Chemical Reagent Co., Ltd. (Shanghai, China). Exo III and 10× Exo III buffer were obtained from Thermo (Shanghai, China). Nb.BbvCI endonuclease and 10× NEBuffer were purchased from New England Biolabs (Beijing, China). All chemical reagents were of analytical grade and used directly without any further purification, and all aqueous solutions were prepared by Milli-Q water (18.2 MΩ cm). Diethyl pyrocarbonate (DEPC)-treated water, SanPrep Column microRNA Extraction Kit, and HPLC-purified DNA were purchased from Sangon Biotechnology Co. (Shanghai, China). HPLC-purified miRNAs were obtained from the Takara Biotechnology Co., Ltd. (Dalian, China). All miRNAs' relevant processes were under the protection of RNase inhibitor. The sequences are shown below:

Components of the buffer solutions used in this work are the following: 10 mM phosphate buffer saline (PBS, pH 7.4), 1× TE buffer (containing 10 mM Tris-HCl, 1.0 mM EDTA), DNA hybridization buffer (containing 1× TE, 1.0 M NaCl, 0.2 mM $MgCl_2$, pH 7.0), 1× NEBuffer 2 (containing 10 mM Tris-HCl, 1.0 mM DDT, 50 mM NaCl, 10 mM $MgCl_2$, pH 7.9).

Scanning electron microscope (SEM) image was obtained by a field emission scanning electron microscope (FESEM, Nova NanoSEM 230, FEI). Transmission electron microscopy (TEM) image was obtained by TEM (Tecnai G2 F20 S-TWIN, FEI, Hillsboro, OR). Powder X-ray diffraction (XRD) spectrum was obtained by using a Bruker D8 Advance X-ray diffractometer. PEC measurements were carried out with a homemade PEC system; a 300-W Xe lamp was used as the irradiation light source. FTO electrode with a fixed valid area

of 0.30 cm^2 served as the working electrode, Pt wire acted as the counter electrode, and Ag/AgCl (KCl-saturated) electrode worked as the reference electrode. Photocurrent was recorded by a CHI660D electrochemical workstation (Shanghai Chenhua, China), with a bias voltage of 0.50 V; PEC tests were carried out in 10 mM PBS.

Synthesis of TiO_2 NPs The preparation of TiO_2 NPs was according to previous reported method with some modifications (see more details in Electronic Supplementary Material, ESI).

Synthesis of hydrogel assembled with TiO_2 NPs Three hundred micromolar amine-modified S1, amine-modified S2, and assistant DNA were mixed in equal volume and hybridized at 37 °C for 2 h. S1 and S2 were hybridized with either end of assistant DNA following base complementary pairing principle, respectively, to form complementary strands (named DNA bridge) with a exposed toehold. 4.0 μL of 10 mg/mL HA and 4.0 μL of 10 mg/mL TiO_2 NP solution were mixed in a centrifuge tube; 1.0 μL of 97.6 mg/mL EDC and 1.0 μL of 23.0 mg/mL NHS were added to activate carboxyl groups of HA for 15 min (solution A). The solution of 2.0 mg/mL PEI and DNA bridge solution were mixed in a volume ratio of 3:5 (solution B). Then, 5.0 μL of solution B was added to the activated solution A, mixed uniformly, and placed in a 37 °C metal bath for 4 h to form target-responsive hydrogel owing to the binding of amine and carboxyl groups. (The synthesis of hydrogels without TiO_2 NPs was almost the same but using buffer instead of TiO_2 NP solution.)

Procedures for miRNA detection Firstly, 50 μL of 2.0 μM HP containing 0.30 U/μL Exo III was mixed with 50 μL of buffer solution containing target in different concentrations; the mixed solution was incubated at 37 °C for 1 h; then, the solution was annealed at 80 °C for 20 min to inactivate the Exo III. Next, the obtained solution and 1.0 μL of 2.5 U/μL Nb.BbvCI were added into the centrifuge tube containing hydrogel and incubated at 37 °C for 2 h. Finally, 90 μL of supernate was collected and added into a customized small cell containing 300 μL of 10 mM PBS for PEC test. (The customized small cylindrical cell has a smaller base area of 1.54 cm^2, which was much smaller than that of usual cells. It can ensure the effective area of the working electrode can be submerged by collected supernatant which in a small volume, which can avoid high dilution of the supernatant.)

Results and discussion

Characterization of prepared TiO_2 NPs and hydrogels The morphology of prepared TiO_2 NPs was characterized by SEM and TEM; the crystal structure was characterized by XRD analysis, which indicated the successful preparation of TiO_2 NPs (see more details in ESI). The hydrogel without TiO_2 NPs and hydrogel embedded with TiO_2 NPs were characterized by SEM. The SEM image of hydrogel without TiO_2 NPs is shown in Fig. 1a, the surface was relatively smooth, while many spherical protuberances could be observed clearly in the SEM image of hydrogel embedded with TiO_2 NPs (Fig. 1b); meanwhile, the morphology and size of those spherical protuberances were consistent with TiO_2 NPs, indicating TiO_2 NPs were embedded in the hydrogels successfully.

Principle of the homogeneous PEC biosensor for miRNA-155 As shown in Scheme 1a, the TiO_2 NP-loaded hydrogel was prepared through the binding of carboxyl groups in HA and amine groups in PEI and DNA bridge. The DNA bridge was the hybridization product of S1, S2, and assistant DNA. S1 and S2 modified with amine group can connect with HA rich in carboxyl group, and the assistant DNA works as a linker for S1 and S2 to form the 3D network structure of hydrogel; more importantly, assistant DNA contains the recognition sequence and nicking site for Nb.BbvCI (the red region). The principle of enzyme-assisted cascaded amplification strategy and the target-responsive mechanism are displayed in Scheme 1b, and the synthetic oligonucleotide sequences are shown in Table 1. HP was designed with a 3′-protruding termini, and containing two functional regions: one part was a target binding domain (the yellow region) which is complementary to the sequence of miRNA-155, another part was a binding domain (the green region) for the exposed toehold, in other words, the single-stranded part of DNA bridge, which contains a recognition sequence (the red region) for the nicking enzyme Nb.BbvCI in the loop of hairpin. In the presence of the target, one part of HP (the yellow region) hybridized with target (miRNA-155) to form double-stranded DNA (dsDNA) and the other part left along. With the help of Exo III, the complementary part (with the target) of HP was hydrolyzed, and the single part of HP was left (named ssDNA). Then, the target was released to hybridize with another HP to initiate the generation of another ssDNA; thus, a lot of ssDNA were obtained thanks to cycle I. After the inactivation of Exo III (Exo III can work on ds DNA, in order to avoid the hydrolyzation effect on DNA bridges in hydrogels to cause high background signal, the Exo III in the solution of cycle I should be inactivated before adding to the centrifuge tube loaded with hydrogel), the resultant solution of cycle I and Nb.BbvCI were added to the centrifuge tube loaded with hydrogel. The ssDNA hybridized with the exposed toehold of DNA bridge in the hydrogel. Since the exposed toehold of DNA bridge had been carefully designed which contains the specific recognition site of the Nb.BbvCI, so DNA bridge was nicked and the ssDNA was released to induce another nick of DNA bridge (cycle II), resulting in the breakage of hydrogel and the release of a lot of signal molecules (TiO_2 NPs) to the supernatant. High photocurrent could be obtained when collected supernatant had

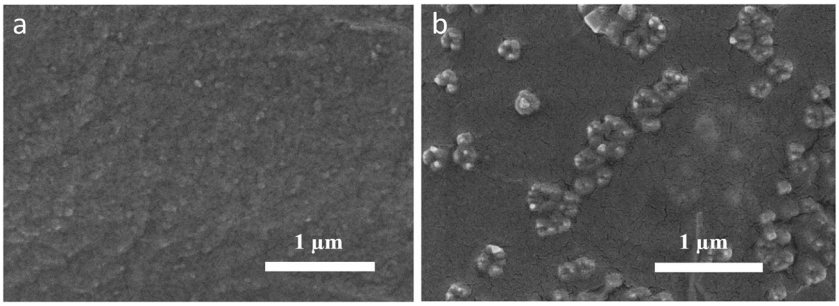

Fig. 1 (a) SEM image of hydrogel without TiO_2 NPs. (b) SEM image of hydrogel embedded with TiO_2 NPs

been applied for PEC test. Since HP was designed with a 3′-protruding termini, which made HP resistant to hydrolyzation by Exo III, consequently, in the absence of the target, the hairpin structure of HP could not be opened, and there was no ssDNA to trigger cycle II, so there was almost no signal molecule released from hydrogel; a low photocurrent was obtained. The photocurrent increased accordingly when the concentration of the target increased. Based on this, a sensitive homogeneous PEC biosensor for miRNA can be developed.

Feasibility test Polyacrylamide gel electrophoresis (12%) experiment was carried out to identify the validity of signal amplification designed in this study realized by Exo III and Nb.BbvCI firstly. Figure 2a shows the results of different samples. The band in lane a corresponded to HP; upon the addition of target, a bright new band with higher molecular weight was observed in lane b, which belonged to HP-target hybrid duplexes; the result proved the successful hybridization of HP and the target. When mixed HP with Exo III (lane

Table 1 Synthetic oligonucleotide sequences*

Name	Sequence (5’→3’)
HP	TGCTAATCGTGATCCTCAGCTTCTATCACGATTAGCATTAA
S1	H_2N-GCGTTGTTCCTTAGC
S2	TCATTAGTCCATATC-NH_2
Assistant DNA	ATGGACTAATGATGTAAGCTGAGGTCAAAAAGGAACAACGC
ssDNA	TGCTAATCGTGATCCTCAGCTT
MiRNA-155	UUAAUGCUAAUCGUGAUAGGGGU
MicroRNA-21	UAGCUUAUCAGACUGAUGUUGA
MiRNA-145	UGGCAGUGUCUUAGCUGGUUGUU
SM-Target	UUAAUGCUAAUCCUGAUAGGGGU
TM-Target	UUAAUUCUAACCGUGACAGGGGU

*The underline letters for HP are the stem of the hairpin structure, the letters marked in green are the output ssDNA sequence, including the letters marked in red which are the recognition sequence for Nb.BbvCI. The underline letters for assistant DNA are the complementary sequence for S1 (right) and S2 (left) and the letters marked in red are the recognition sequence and nicking site for Nb.BbvCI. The letters marked in red for SM-Target and TM-Target are the bases which differ from those in miRNA-155

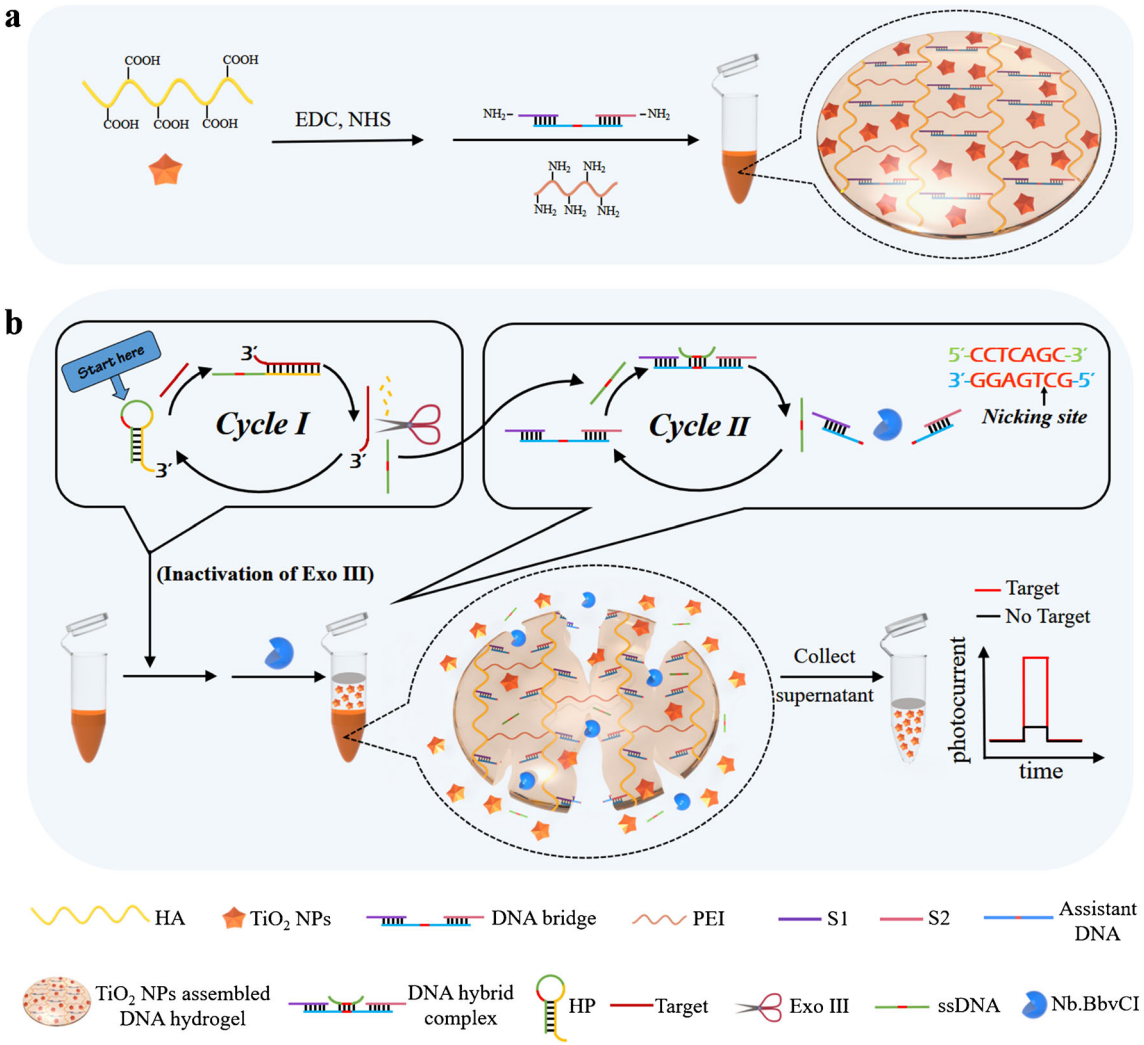

Scheme 1 (a) The diagram of the construction of TiO_2-embedded hydrogel. (**b**) The principle of the proposed homogeneous PEC sensor for miRNA-155 based on target-responsive hydrogel coupled with Exo III and Nb.BbvCI assistant cascaded amplification strategy

c), the band showed no difference with HP alone (lane a), indicating that HP was free from digestion by Exo III in the absence of target due to its 3′-protruding termini. After adding the target, the band of HP-target hybrid duplexes becomes obviously dark in lane d compared with that in the absence of target (lane b), indicating the digestion effect of Exo III to the HP-target hybrid duplexes. Meanwhile, a new band with smaller molecular weight appeared in lane d, which verified the generation of ssDNA in the presence of target; these results confirmed the actual occurrence of cycle I. Lane g presents successful hybridization of S1, S2, and assistant DNA to form DNA bridge. Lane h shows the hybridization of DNA bridge with ssDNA (bought from Sangon Biotechnology Co.) to DNA hybrid complex. Upon addition of Nb.BbvCI, the band of ssDNA-DNA bridge hybrid structure becomes faded in lane i, confirming the nicking effect of Nb.BbvCI to ssDNA-DNA bridge hybrid structure, and the new band with smaller molecular weight corresponded to two nicked fragments of DNA bridge. Lane e is the control group (without target); a dim band in the same position with nicked fragments was produced, which may be due to a little unwished DNA hybridization or non-specific cleavage of DNA enzymes. Lane f is the experimental group (with target); the band in the same position with nicked fragments was much more brilliant than the control, confirming the occurrence of cycle II. These results indicated the feasibility of Exo III and Nb.BbvCI-based cascaded amplification strategy.

Then, simple experiments had been performed to verify the feasibility of the PEC biosensor for miRNA detection. As shown in Fig. 2b, a small PEC signal was detected because of little leakage of TiO_2 NPs if only buffer solution was added into the centrifuge tube loaded with hydrogel. The photocurrent of the control group (without target, other components were the same with the experimental group) was little higher

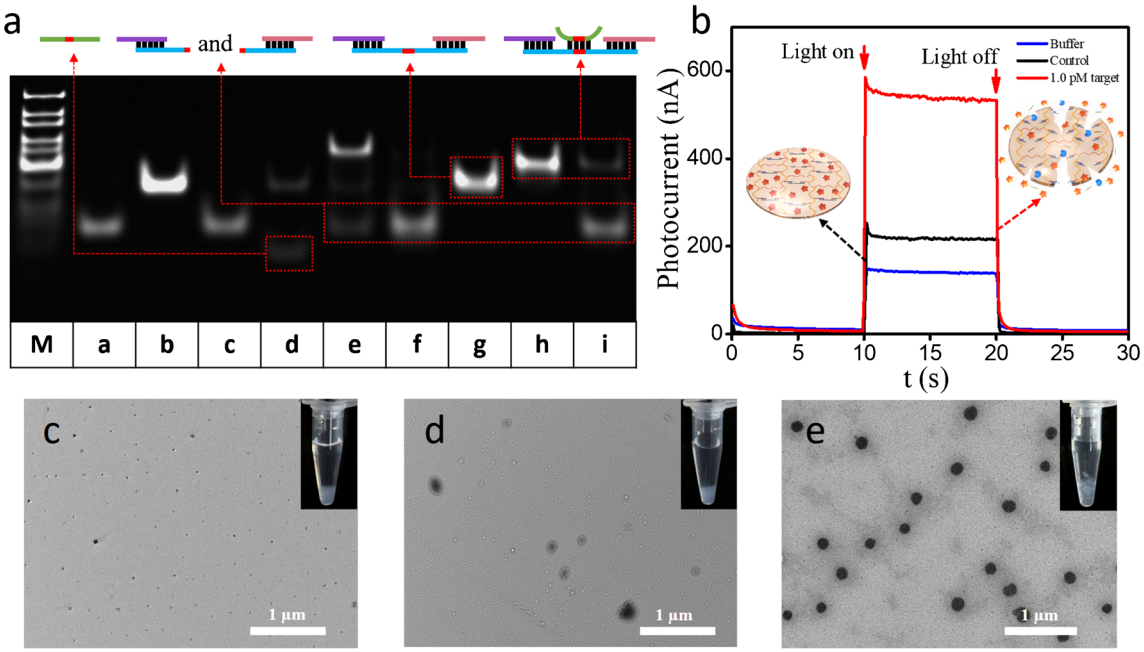

Fig. 2 (a) 12% gel electrophoresis image of HP (lane a), HP + target (lane b), HP + Exo III (lane c), lane c + target (lane d), lane c + S1 + S2 + assist + Nb.BbvCI (lane e), lane e + target (lane f), S1 + S2 + A (lane g), lane g + ssDNA (lane h), and lane h + Nb.BbvCI (lane i); the concentrations of all DNA and the target were 2.0 μM, and the concentrations of Exo III and Nb.BbvCI were 0.15 U/μL and 0.025 U/μL, respectively. (b) PEC tests for supernate from different samples (PEC tests were carried out in 10 mM PBS, pH 7.4, a Xe lamp was used as the irradiation light source, with a bias voltage of 0.50 V). The TEM images of collected supernate when adding buffer (c), the solution of cycle 1 in the absence of the target (d), and the solution of cycle 1 in the presence of 10 pM target (e) into the centrifuge tubes loaded with hydrogel, respectively; the inset pictures were the physical pictures of each sample

than that of buffer solution; this may be due to little unwished hybridization of DNA or non-specific cleavage of DNA enzymes. In the presence of 1.0 pM target, the photocurrent intensity of the experimental group increased significantly compared to the control, which was on account of the target-induced nicking of DNA bridge, resulting in the breakage of hydrogel and the release of TiO_2 NPs. These results demonstrated the feasibility of the proposed biosensor. The corresponding supernate was characterized by TEM, as shown in Fig. 2c; when only buffer solution was added into the centrifuge tube loaded with hydrogel, few TiO_2 NPs whose diameter was less than 30 nm (which was too small and escaped from the hydrogel) and some inorganic salt crystals in buffer can be observed in the TEM image of the supernate. In the absence of the target, there were few TiO_2 NPs that can be observed (Fig. 2d), which may due to the non-specific cleavage of DNA enzymes. In the presence of the target, a lot of TiO_2 NPs can be clearly seen in the TEM image (Fig. 2e), whose morphology and size were consistent with those in Fig. 1a and 1b. As shown in the physical pictures (inset pictures in Fig. 2c, Fig. 2d, and Fig.2e), the hydrogels still maintained their intact morphology in Fig. 2c and Fig. 2d; while the structure of hydrogel in Fig. 2e was damaged, the intact structure became loose and scattered. These results verified the breakage of hydrogels and the release of TiO_2 NPs in the presence of the target.

Analytical performance of the proposed system To assess the analytical performance of the proposed biosensor for miRNA-155 detection, a series of samples containing various concentrations of target were tested under the optimized conditions (see more details in ESI). As displayed in Fig. 3a, with the increase of target concentration, the value of the photocurrent increased synchronously. And there is a good linear relationship between photocurrent value (I) and the logarithmic concentration of the target (C_{target}) from 1.0 fM to 100 pM (shown in Fig. 3b). The linear equation is:

$$I\ (\mathrm{nA}) = 103.83\ \mathrm{Log}\ C_{target}\ (\mathrm{pM}) + 535.44$$

The correlation coefficient (R^2) is 0.991 and the limit of detection (LOD) is 0.41 fM ($S/N = 3$). The performance of the proposed PEC sensor was compared with other methods for miRNA detection; the prepared biosensor showed a wider linear range or lower LOD compared to previous homogeneous PEC sensors for miRNA. [11, 12] As displayed in Table 2, the low LOD and the wide linear range of this sensor were superior or comparable to previous studies for miRNA detection based on different methods.

Several similar targets including single-base mismatched target (SM-Target), three-bases mismatched target (TM-Target), miRNA-21, and miRNA-145 had been chosen as model interferents (the concentration of which was 10 pM while the

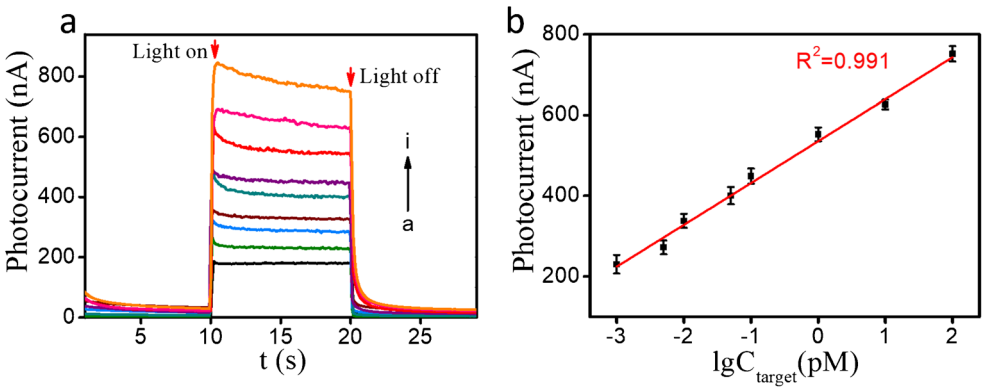

Fig. 3 (a) The PEC signal of the target at various concentrations, a to i: control (0), 1.0 fM, 5.0 fM, 10 fM, 50 fM, 100 fM, 1.0 pM, 10 pM, 100 pM. (b) Linear plot of PEC signal vs logarithmic concentration of the target (R^2 = 0.991)

target concentration was 1.0 pM) to investigate the selectivity of the developed sensor. As displayed in Fig. 4a, the SM-Target and TM-Target caused a slight increase in photocurrent. The signals after the addition of miRNA-21 and miRNA-145 had no obvious difference compared to that from the control. When mixed miRNA-21 and miRNA-145 with the target (mix), the photocurrent intensity was almost the same with the target alone; these results indicated that the proposed PEC sensor had good selectivity and anti-interference performance.

To explore the reproducibility of the proposed biosensor, five hydrogels in the same batch (intra-assay) and five hydrogels in different batches (inter-assay) were utilized to detect 1.0-pM target. The relative standard deviation (RSD) of photocurrent intensity of five hydrogels in the same batch was 2.7%, while the RSD of photocurrent intensities of five hydrogels in different batches was 3.0%, indicating that the proposed sensing platform had good reproducibility (shown in Fig. 4b). The stability analysis of the biosensor is shown in Fig. 4c, the photocurrent response after 12 cycles of on/off irradiation still remains 96.4% of the initial value (for 10 pM target), indicating that the biosensor had good stability. The storage stability of prepared target-responsive hydrogels was also investigated. Hydrogels were stored at 4 °C for 1 to 4 weeks, respectively, and the photocurrent (for 10 pM target) obtained by those hydrogels had no obvious difference with that by fresh hydrogels (Fig. 4d), indicating that prepared hydrogels had good storage stability.

Real sample analysis The developed biosensor was applied to detect the target in HeLa (human cervical carcinoma cell line), MCF-7 (human breast cancer cell line), HUCEC (human normal cervical cell line), and MCF-10A (human normal breast epithelial cell line) cell lysates, where HUCEC and MCF-10A were used as control, respectively (the experimental details are given in ESI). As displayed in Fig. S3, the photocurrent increased gradually with the increase of cell number. Furthermore, the detected concentrations of the target in Hela cells were calculated to be 7.32 fM, 39.16 fM, and 475.52 fM when the cell number was 10^2, 10^3, and 10^4, respectively, while the concentrations of the target in MCF-7 were 1.52 fM, 12.32 fM, and 162.49 fM, when the cell number was 10^2, 10^3, and 10^4, respectively; the photocurrent intensities of miRNA extracted from HeLa and MCF-7 had obvious enhancements compared to their control groups, which was consistent with the up-regulated level of target in these two kinds of cells [3], which revealed that the proposed PEC sensor had the potential in monitoring miRNA in cancer cells. To evaluate the accuracy of the method, the recovery experiment in spiked blank sample (1× NEBuffer 2) had been carried

Table 2 Comparison of the developed PEC biosensor with other strategies for miRNA detection

Method	Dynamic range (fM to nM)	Detection limit (fM)	References
Electrochemistry	100 to 1.0	33	[27]
Electrochemistry	1.0 to 1.0	0.46	[28]
Electrochemiluminescence	100 to 0.10	33	[29]
Electrochemiluminescence	5.0 to 0.0050	0.5	[30]
PEC	1.0 to 1.0	0.26	[31]
PEC	200 to 25	65	[12]
PEC	2.0 to 0.17	0.6	[32]
PEC	1.0 to 0.10	0.41	This work

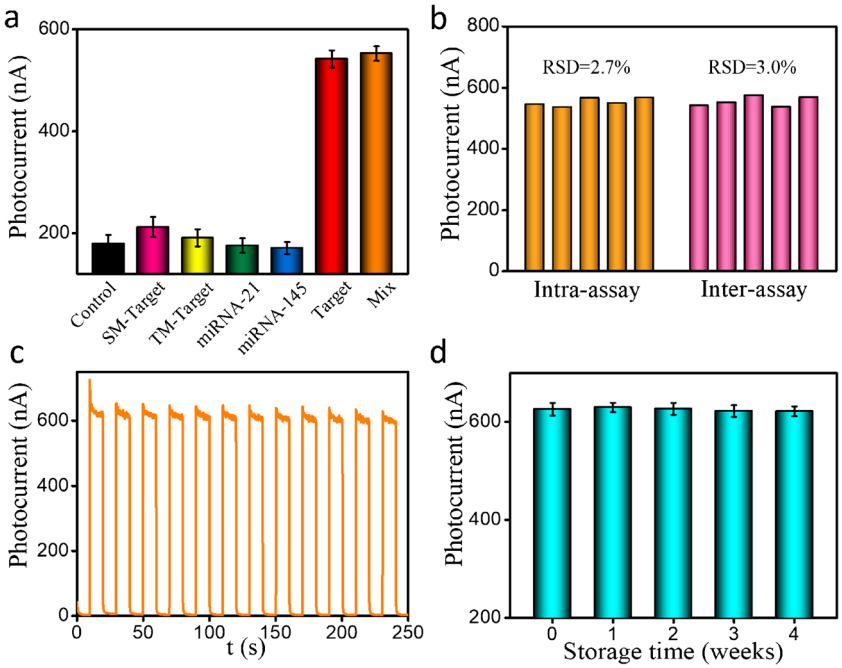

Fig. 4 (a) Selectivity and (b) reproducibility analysis of the proposed biosensor, (**c**) the photocurrent responses under several on/off irradiation cycles, (**d**) the storage stability of prepared hydrogels

out; the results are shown in Table S1, the recoveries in the range of 98.5 to 103.8%, with the relative standard deviation (RSD) from 2.7 to 3.9%; these results demonstrated the accuracy of proposed PEC assay and suggested its potential for real sample monitoring.

Conclusion

A sensitive homogeneous PEC biosensor for miRNA detection has been developed based on TiO_2 NP-equipped hydrogels and cascade signal amplification. With the help of Exo III and Nb.BbvCI, the sensitivity of the biosensor was improved enough to meet the real sample test requirement. The proposed biosensor circumvented the tedious procedures of electrode modification and exhibited the advantages of simpleness, speediness, and good reproducibility. The prepared hydrogels have long time storage stability, which can be prepared in advance and save time during test. By simply changing the sequence of HP and DNA bridge, detection of many different targets can be easily realized.

Supplementary Information The online version contains supplementary material available at https://doi.org/10.1007/s00604-021-04935-6.

Funding This project was financially supported by the National Key Research and Development Program of China (No. 2019YFC1604701), National Sciences Foundation of China (21974020, 21775026) and the cooperative project of production and study in University of Fujian Province (2018Y4007), the Sciences Foundation of Fujian Province (2018 J01685, 2018J01682), and the United Fujian Provincial Health and Education Project for Tackling the Key Research P. R. China (2019-WJ-11).

Declaration

Conflict of interest The authors declare no competing interests.

References

1. Lu J, Getz G, Miska EA, Alvarez-Saavedra E, Lamb J, Peck D, Sweet-Cordero A, Ebert BL, Mak RH, Ferrando AA, Downing JR, Jacks T, Horvitz HR, Golub TR (2005) MicroRNA expression profiles classify human cancers. Nature 435:834–838. https://doi.org/10.1038/nature03702
2. Calin GA, Croce CM (2006) MicroRNA signatures in human cancers. Nat Rev Cancer 6:857–866. https://doi.org/10.1038/nrc1997
3. Lu Y, Xiao J, Lin H, Bai Y, Luo X, Wang Z, Yang B (2009) A single anti-microRNA antisense oligodeoxyribonucleotide (AMO) targeting multiple microRNAs offers an improved approach for microRNA interference. Nucleic Acids Res 37:e24. https://doi.org/10.1093/nar/gkn1053
4. Li J, Yao B, Huang H, Wang Z, Sun C, Fan Y, Chang Q, Li S, Wang X, Xi J (2009) Real-time polymerase chain reaction microRNA detection based on enzymatic stem-loop probes ligation. Anal Chem 81:5446–5451. https://doi.org/10.1021/ac900598d
5. Valoczi A, Hornyik C, Varga N, Burgyan J, Kauppinen S, Havelda Z (2004) Sensitive and specific detection of microRNAs by northern blot analysis using LNA-modified oligonucleotide probes. Nucleic Acids Res 32:e175. https://doi.org/10.1093/nar/gnh171
6. Lim LP, Lau NC, Garrett-Engele P, Grimson A, Schelter JM, Castle J, Bartel DP, Linsley PS, Johnson JM (2005) Microarray analysis shows that some microRNAs downregulate large numbers of target mRNAs. Nature 433:769–773. https://doi.org/10.1038/nature03315
7. Fu N, Wang L, Zou X, Li C, Zhang S, Zhao B, Gao Y, Wang L (2020) A photoelectrochemical sensor based on a reliable basic photoactive matrix possessing good analytical performance for miRNA-21 detection. Analyst 145:7388–7396. https://doi.org/10.1039/d0an01297a

8. Yu LD, Wen YX, Zhang XY, Li NB, Luo HQ (2020) Signal-off photoelectrochemical determination of miRNA-21 using aptamer-modified In2O3@Cu2MoS4 nanocomposite. Mikrochim Acta 187: 561. https://doi.org/10.1007/s00604-020-04540-z
9. Huang X, Liu Y, Yung B, Xiong Y, Chen X (2017) Nanotechnology-enhanced no-wash biosensors for in vitro diagnostics of cancer. ACS Nano 11:5238–5292. https://doi.org/10.1021/acsnano.7b02618
10. Hong Q, Ge L, Wang W, Liu X, Li F (2018) Oligonucleotide-modulated photocurrent enhancement of a tetracationic porphyrin for label-free homogeneous photoelectrochemical biosensing. Biosens Bioelectron 121:90–95. https://doi.org/10.1016/j.bios.2018.08.071
11. Hou T, Xu N, Wang W, Ge L, Li F (2018) Truly immobilization-free diffusivity-mediated photoelectrochemical biosensing strategy for facile and highly sensitive microRNA assay. Anal Chem 90: 9591–9597. https://doi.org/10.1021/acs.analchem.8b02523
12. Song X, Hou T, Lu F, Wang Y, Liu J, Li F (2020) Homogeneous photoelectrochemical biosensing via synergy of G-quadruplex/hemin catalysed reactions and the inner filter effect. Chem Commun (Camb) 56:1811–1814. https://doi.org/10.1039/c9cc09280c
13. Wu J, Lv W, Yang Q, Li H, Li F (2021) Label-free homogeneous electrochemical detection of MicroRNA based on target-induced anti-shielding against the catalytic activity of two-dimension nanozyme. Biosens Bioelectron 171:112707. https://doi.org/10.1016/j.bios.2020.112707
14. Li H, Chang J, Gai P, Li F (2018) Label-free and ultrasensitive biomolecule detection based on aggregation induced emission fluorogen via target-triggered hemin/G-quadruplex-catalyzed oxidation reaction. ACS Appl Mater Interfaces 10:4561–4568. https://doi.org/10.1021/acsami.7b18676
15. Wu J, Yang Q, Li Q, Li H, Li F (2021) Two-dimensional MnO2 nanozyme-mediated homogeneous electrochemical detection of organophosphate pesticides without the interference of H2O2 and color. Anal Chem 93:4084–4091. https://doi.org/10.1021/acs.analchem.0c05257
16. Um SH, Lee JB, Park N, Kwon SY, Umbach CC, Luo D (2006) Enzyme-catalysed assembly of DNA hydrogel. Nat Mater 5:797–801. https://doi.org/10.1038/nmat1741
17. Miyata T, Jige M, Nakaminami T, Uragami T (2006) Tumor marker-responsive behavior of gels prepared by biomolecular imprinting. Proc Natl Acad Sci U S A 103:1190–1193. https://doi.org/10.1073/pnas.0506786103
18. Lin Y, Wang X, Sun Y, Dai Y, Sun W, Zhu X, Liu H, Han R, Gao D, Luo C (2019) A chemiluminescent biosensor for ultrasensitive detection of adenosine based on target-responsive DNA hydrogel with Au@HKUST-1 encapsulation. Sensors Actuators B Chem 289:56–64. https://doi.org/10.1016/j.snb.2019.03.075
19. He Y, Yang X, Yuan R, Chai Y (2017) Switchable target-responsive 3D DNA hydrogels as a signal amplification strategy combining with SERS technique for ultrasensitive detection of miRNA 155. Anal Chem 89:8538–8544. https://doi.org/10.1021/acs.analchem.7b02321
20. Yan L, Zhu Z, Zou Y, Huang Y, Liu D, Jia S, Xu D, Wu M, Zhou Y, Zhou S, Yang CJ (2013) Target-responsive "sweet" hydrogel with glucometer readout for portable and quantitative detection of non-glucose targets. J Am Chem Soc 135:3748–3751. https://doi.org/10.1021/ja3114714
21. Tan B, Zhao H, Du L, Gan X, Quan X (2016) A versatile fluorescent biosensor based on target-responsive graphene oxide hydrogel for antibiotic detection. Biosens Bioelectron 83:267–273. https://doi.org/10.1016/j.bios.2016.04.065
22. Liu D, Jia S, Zhang H, Ma Y, Guan Z, Li J, Zhu Z, Ji T, Yang CJ (2017) Integrating target-responsive hydrogel with pressuremeter readout enables simple, sensitive, user-friendly, quantitative point-of-care testing. ACS Appl Mater Interfaces 9:22252–22258. https://doi.org/10.1021/acsami.7b05531
23. Zhu Z, Guan Z, Jia S, Lei Z, Lin S, Zhang H, Ma Y, Tian ZQ, Yang CJ (2014) Au@Pt nanoparticle encapsulated target-responsive hydrogel with volumetric bar-chart chip readout for quantitative point-of-care testing. Angew Chem Int Ed Engl 53:12503–12507. https://doi.org/10.1002/anie.201405995
24. Zhao M, Wang P, Guo Y, Wang L, Luo F, Qiu B, Guo L, Su X, Lin Z, Chen G (2018) Detection of aflatoxin B1 in food samples based on target-responsive aptamer-cross-linked hydrogel using a hand-held pH meter as readout. Talanta 176:34–39. https://doi.org/10.1016/j.talanta.2017.08.006
25. Li Z, Zhang J, Chen H, Huang X, Huang D, Luo F, Wang J, Guo L, Qiu B, Lin Z (2019) Electrochemiluminescence biosensor for hyaluronidase based on the Ru(bpy)32+ doped SiO2 nanoparticles embedded in the hydrogel fabricated by hyaluronic acid and polyethylenimine. ACS Applied Bio Materials 3:1158–1164. https://doi.org/10.1021/acsabm.9b01082
26. Huang Y, Ma Y, Chen Y, Wu X, Fang L, Zhu Z, Yang CJ (2014) Target-responsive DNAzyme cross-linked hydrogel for visual quantitative detection of lead. Anal Chem 86:11434–11439. https://doi.org/10.1021/ac503540q
27. Wang J, Hui N (2019) Electrochemical functionalization of polypyrrole nanowires for the development of ultrasensitive biosensors for detecting microRNA. Sensors Actuators B Chem 281:478–485. https://doi.org/10.1016/j.snb.2018.10.131
28. Ren R, Bi Q, Yuan R, Xiang Y (2020) An efficient, label-free and sensitive electrochemical microRNA sensor based on target-initiated catalytic hairpin assembly of trivalent DNAzyme junctions. Sensors and Actuators B-Chemical 304. https://doi.org/10.1016/j.snb.2019.127068
29. Zhu HY, Ding SN (2019) Dual-signal-amplified electrochemiluminescence biosensor for microRNA detection by coupling cyclic enzyme with CdTe QDs aggregate as luminophor. Biosens Bioelectron 134:109–116. https://doi.org/10.1016/j.bios.2019.04.005
30. Kerr E, Farr R, Doeven EH, Nai YH, Alexander R, Guijt RM, Prieto-Simon B, Francis PS, Dearnley M, Hayne DJ, Henderson LC, Voelcker NH (2021) Amplification-free electrochemiluminescence molecular beacon-based microRNA sensing using a mobile phone for detection. Sensors Actuators B Chem 330:129261. https://doi.org/10.1016/j.snb.2020.129261
31. Yi W, Cai R, Xiang D, Wang Y, Zhang M, Ma Q, Cui Y, Bian X (2019) A novel photoelectrochemical strategy based on an integrative photoactive heterojunction nanomaterial and a redox cycling amplification system for ultrasensitive determination of microRNA in cells. Biosens Bioelectron 143:111614. https://doi.org/10.1016/j.bios.2019.111614
32. Li L, Zhang Y, Yan Z, Chen M, Zhang L, Zhao P, Yu J (2020) Ultrasensitive photoelectrochemical detection of microRNA on paper by combining a cascade nanozyme-engineered biocatalytic precipitation reaction and target-triggerable DNA motor. ACS Sensors 5:1482–1490. https://doi.org/10.1021/acssensors.0c00632